

High-Throughput Screening of Earth-Abundant Water Reduction Catalysts toward Photocatalytic Hydrogen Evolution

Rachel N. Motz, Eric M. Lopato, Timothy U. Connell, and Stefan Bernhard*

Cite This: *Inorg. Chem.* 2021, 60, 774–781

Read Online

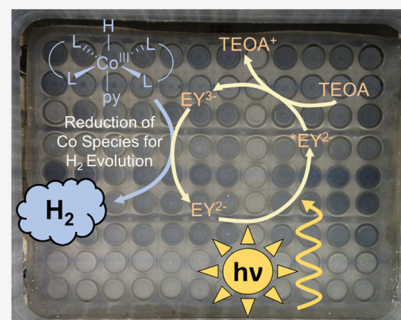
ACCESS |

Metrics & More

Article Recommendations

Supporting Information

ABSTRACT: Noble-metal photosensitizers and water reduction co-catalysts (WRCs) still present the highest activity in homogeneous photocatalytic hydrogen production. The search for earth-abundant alternatives is usually limited by the time required to screen new catalyst combinations; however, here, we utilize newly designed and developed high-throughput photoreactors for the parallel synthesis of novel WRCs and colorimetric screening of hydrogen evolution. This unique approach allowed rapid optimization of photocatalytic water reduction using the organic photosensitizer Eosin Y and the archetypal cobaloxime WRC [Co(GL1)₂pyCl], where GL1 is dimethylglyoxime and py is pyridine. Subsequent combinatorial synthesis generated 646 unique cobalt complexes of the type [Co(LL)₂pyCl], where LL is a bidentate ligand, that identified promising new WRC candidates for hydrogen production. Density functional theory (DFT) calculations performed on such cobaloxime derivative complexes demonstrated that reactivity depends on hydride affinity. Alkyl-substituted glyoximes were necessary for hydrogen production and showed increased activity when paired with ligands containing strong hydrogen-bond donors.



INTRODUCTION

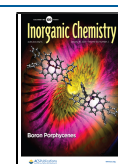
Society is faced with an increasing demand for energy, leading to a push for sustainable or renewable alternatives. Despite the increasing implementation of electricity generated via solar, hydro, and wind power, chemical fuels continue to rely on carbon-based sources. Storage and transport of these feedstocks is critical in sectors like transportation and manufacturing, but their use also leads to substantial emissions; 66% of global greenhouse gas emissions result from industrial processes, powering transportation, or producing heat and electricity.¹ Hydrogen is an emerging alternative to replace fossil fuels; in addition to its high calorific value and sole combustion product of water, it is also an important feedstock in oil refining and ammonia fixation.² It is therefore unfortunate that hydrogen production is currently sustained primarily by steam reforming, which is extremely carbon-intensive: every metric ton of hydrogen produced results in almost seven metric tons of carbon dioxide.³

Photocatalytic water reduction presents a carbon-emission-free method for generating hydrogen.^{4,5} This homogeneous process requires only three molecular components: a photosensitizer to capture light and convert it to chemical energy, a water reduction co-catalyst (WRC) to drive the redox reaction, and an organic sacrificial donor to supply electrons. The majority of reported photocatalytic systems utilize noble-metal photosensitizers, commonly made from iridium(III), rhenium(I), rhodium(III), ruthenium(II), and platinum(II).^{6–10} While these typically demonstrate high activity and efficiency, the rarity, expense, and toxicity of noble metals necessitate the search for more sustainable alternatives. Luminescent organic

dyes, such as Eosin Y (EY) (Figure 1a), are significantly cheaper than metal-based phosphors and also exhibit photo-physics amenable to both synthetic photochemistry^{11,12} and water reduction.^{13–16} Co-catalysts with the highest turnover also contain noble metals, especially colloidal platinum and palladium, but they can also be replaced with earth-abundant alternatives, particularly molecular complexes of cobalt, iron, and nickel.^{10,17} Specifically, there is a great variety in reported cobalt complexes with ligand derivatives that include 2,2'-bipyridine, glyoxime, dithiolene,¹⁷ macrocycles,¹⁸ and Schiff bases.¹⁹ The facile redox chemistry that allows cobalt to transition between its +3 and +1 oxidation states in single-electron steps enables a variety of potential mechanistic pathways; water is reduced either by monomolecular protonation of cobalt(III or II) hydride or by a bimolecular pathway, where two cobalt(III) hydrides react to evolve H₂ (Figure 1b).^{17–20} Multiple proposed mechanisms for this catalyst moiety are still debated in the literature.^{15,20–30} Computational work has also provided support for the particular order of reaction intermediates and shed light on potential rate-limiting steps for electrocatalytic water reduction involving cobalt species.^{21,31} Cobaloxime complexes that

Received: September 18, 2020

Published: January 7, 2021



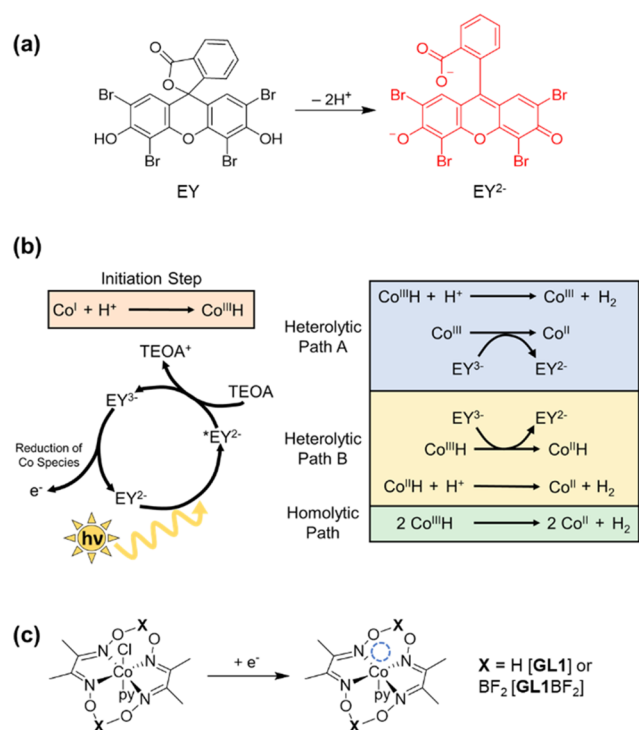


Figure 1. (a) Structure of Eosin Y in its neutral and photoactive anionic form. (b) Reported mechanisms for light-driven water reduction using Eosin Y and cobalt catalyst. Note that an oxidative quenching pathway for Eosin Y involving Co species is often also discussed. (c) Structure of cobaloxime water reduction co-catalyst.

contain two bidentate dimethylglyoximes (GL1) and an axial monodentate ligand (commonly pyridine, py), particularly [Co(GL1)₂pyCl] and the difluoroborylated derivative [Co(GL1BF₂)₂pyCl] (Figure 1c), are robust water reduction co-catalysts known to evolve hydrogen in combination with noble-metal^{7,32} and organic dye^{15,16,30} photosensitizers. Some variations of the glyoxime ligand structure have also been tested including a formal tetradentate diimine-dioxime architecture generated by alkyl bridging^{26,33} and bioinspired tethering of the glyoxime and photosensitizer moieties.³⁴

Optimization of a single reaction ($2\text{H}^+ + 2\text{e}^- \rightarrow \text{H}_2$) has predicated extensive ad hoc screening of new WRC candidates;^{10,17} however, the large variety in reported assay conditions makes comparison of promising candidates difficult.³⁵ Parallelized, high-throughput experimentation provides a standardized platform that enables the optimization of multiple reaction parameters and rapid combinatorial screening for novel catalysts. These advantages, particularly along with big data analysis, drive the continued uptake of a high-throughput approach in fields as diverse as biocatalytic activity, pharmaceutical synthesis, and toxicology.^{36–38} Combinatorial synthesis has been applied to the discovery of new heterogeneous photocatalysts including TiO₂ nanoparticles³⁹ and conjugated organic polymers,⁴⁰ but it is still limited by the need for costly automated equipment and characterization platforms. Computational screening does not require expensive experimental infrastructure, and theoretical analyses of large calculated property libraries have identified promising candidates of nitride, oxynitride, and oxide photocatalysts for heterogeneous water splitting.^{41,42} These simulations, while providing some predictive capability, still incur inherent

computational costs and do not diminish the need for large experimental datasets.

Expanding on our recent effort to design more affordable high-throughput experimentation for photocatalytic water reduction,^{43,44} here, we report the first application of parallel synthesis and screening in a homogeneous catalytic system that contains no noble-metal components. Newly designed and developed photoreactors allowed rapid optimization of varied reaction conditions including concentration of each component, water fraction, and solution pH. Earth-abundant WRCs based on the cobaloxime scaffold were synthesized *in situ*, avoiding the need for traditional batch synthesis and enabling the generation of a structurally diverse combinatorial library with tunable activity.⁴⁵ Computational modeling allowed the exploration of the structure–activity relationship for bis-glyoxime complexes and to determine the energy changes of reaction steps that dictate catalytic activity. Hydrogen production across this library was monitored using a chemoselective, colorimetric tape and identified promising new WRC candidates with higher reactivity than the parent [Co(GL1)₂pyCl] complex.

EXPERIMENTAL SECTION

Synthesis of Glyoxime Derivate Ligands. All reagents and solvents were commercially sourced and used without further purification. Nuclear magnetic resonance (NMR) spectra were obtained using a 500 Bruker Avance III or a 500 Bruker Avance Neo spectrometer (¹H, 500 MHz; ¹³C, 125.8 MHz); spectra were referenced to residual solvent peaks. Ligands GL1,⁴⁶ NH1,⁴⁷ NH2,⁴⁸ NH3,⁴⁹ and NH4⁵⁰ and cobalt complexes [Co(GL1)₂pyCl] and [Co(GL1BF₂)₂pyCl]⁵¹ were synthesized according to previously reported procedures. Detailed synthetic procedures and characterization are provided in the Supporting Information.

Optimization Reactions. Homogeneous photocatalytic water reduction reactions were performed in photoreactors designed and developed (Figure 2) in our laboratory:³⁴ the organic dye Eosin Y



Figure 2. (a) White LED strips and camera attached to a plexiglass cage for monitoring reaction progress; (b) 108 reaction vials (1 mL) covered in H₂-sensitive colorimetric tape sealed with silicone and plexiglass; (c) two 100 W blue LED chips (440 ± 10 nm).

(EY) served as a photosensitizer in a mixture of 2-ethoxyethanol and water with a large excess of triethanolamine (TEOA) as sacrificial reductant. Reactions were irradiated for at least 16 h using blue light-emitting diodes (LEDs) (440 ± 10 nm), and progress was monitored via time lapse photography (10 min intervals) of a commercially available colorimetric tape sensitive to hydrogen. Reaction vials contained a total solution volume of 650 μL. The change in color of the hydrogen-sensitive tape was digitized using a Mathematica script and plotted vs reaction time. The cobalt-based WRC [Co(GL1BF₂)₂pyCl], selected for its stability and performance,^{16,24,25}

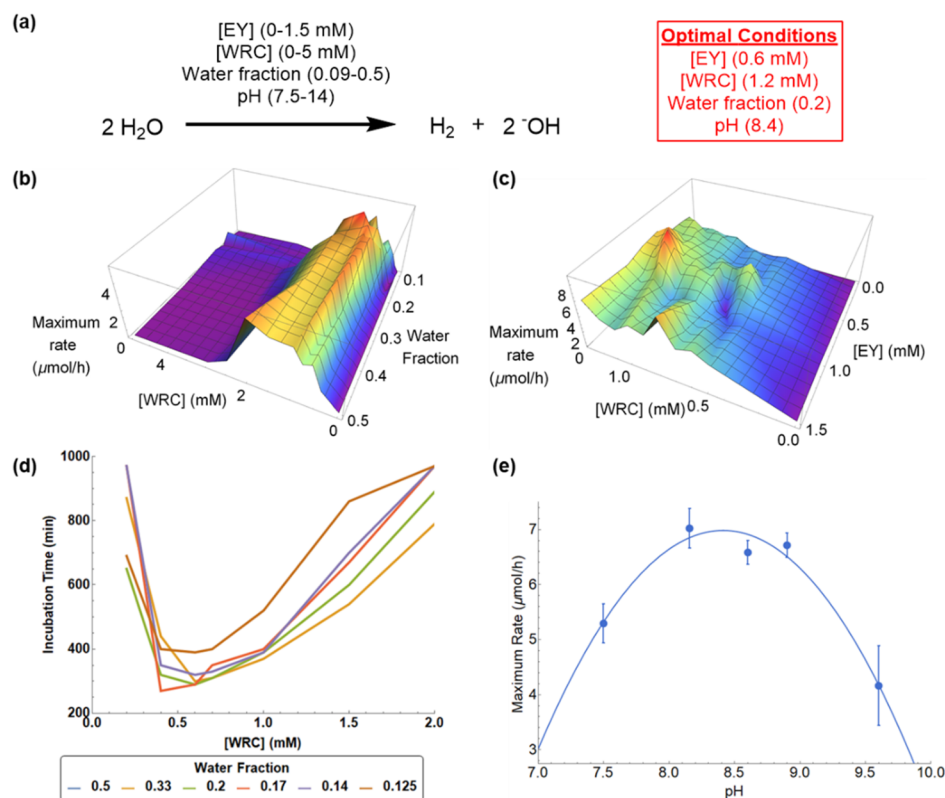


Figure 3. (a) Optimal conditions for high-throughput photocatalytic water reduction to hydrogen gas; surface plots of maximum rates for (b) water fraction vs WRC and (c) EY vs WRC; (d) series of WRC concentrations at water fractions demonstrating the dependence of incubation time on the WRC content; and (e) pH dependence of hydrogen evolution, with error bars representing the standard deviation of four different WRC concentrations, and quadratic fit $R^2 > 0.99$.

was used to determine optimal reaction conditions, including water fraction, concentration of each component, and pH. Optimal reaction conditions were determined by the calculation of the maximum rate of hydrogen production (Figure 3a).

Parallelized Catalyst Screening. Novel WRC complexes were synthesized *in situ* and screened via our photoreactors. Appropriate equivalents of cobalt chloride, ligand, and pyridine solutions in 2-ethoxyethanol (total volume, 520 μL) were sequentially added in aliquots to reaction vials and allowed to stand for 10 min. Subsequently, EY in solution with 30% TEOA in water (130 μL) was added via a pipette and photocatalytic reactions were monitored by photography every 10 min for a total of 1000 min.

RESULTS AND DISCUSSION

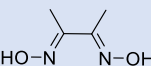
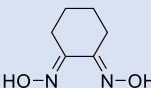
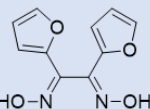
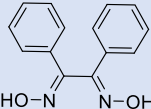
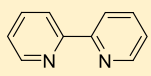
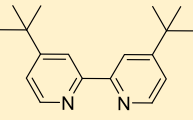
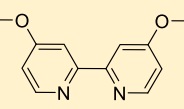
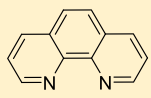
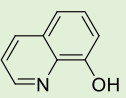
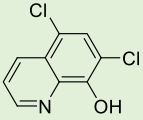
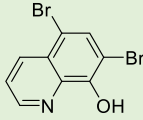
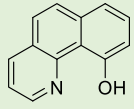
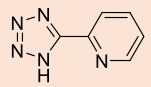
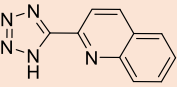
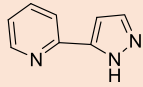
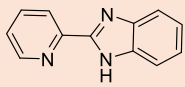
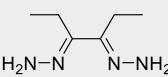
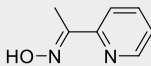
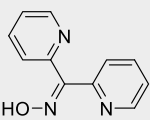
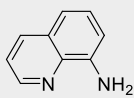
Optimization of Photocatalytic Water Reduction.

Homogeneous water reduction typically requires organic solvents to ensure catalyst solubility but can result in a low water content.^{8,9} The system developed here utilized a solvent mixture of ethoxyethanol and water; ethoxyethanol served as a proxy for ethanol, in which cobaloximes are typically synthesized, but with a higher boiling point to avoid detection issues. Although EY demonstrates solvatochromism, the absorption of EY in water vs that in ethanol differs minimally.^{52,53} First, we tested the correlation between water content and WRC concentration on hydrogen production (Figures 3b and S1). Lower concentrations of WRC performed better with a smaller water fraction, and higher concentrations were similarly optimal with a greater water content. Although not the only factor responsible for strong performance, conditions with the highest performance centered around a catalyst/water ratio of approximately 1:7000 molecules (Figure

S2). The incubation time before hydrogen was detected ranged from 200 to 900 min depending on sample conditions (see the Supporting Information for details). The shortest incubation times were observed at a relatively low WRC concentration (0.4–0.8 mM) regardless of the water fraction (Figure 3d), and we speculate that this might represent the time required to generate the active catalyst species (Figure 1b). Given the complexity of the surfaces observed in these experiments (Figure 3b,c), various combinations of proposed mechanisms likely contribute to the activity differently based on reaction conditions. The correlation between hydrogen production and water-to-cobalt ratio revealed a similar parabolic relationship, with minimal incubation times at ratios of 10 000–20 000 (Figure S2). Overall, limited hydrogen was produced at both large and small molar equivalents of water; we rationalize the lower activity at small molar ratios by the decreased likelihood of catalyst/substrate interaction. Nevertheless, hydrogen was produced even when the water content was increased up to 0.5, demonstrating a reduced reliance on organic solvents that is more representative of commercially relevant conditions. Water fraction was fixed at 0.2 in further experiments as it provided the highest activity across the broadest WRC concentration range.

The WRC exhibited an effective working range between 0.2 and 2 mM, assuming a fixed EY concentration, and reached peak activity at approximately 1 mM. Outside this range, little to no hydrogen production was detected. Hydrogen produced at low catalyst concentrations (<0.2 mM) is likely below the system's limit of detection. Conversely, at high concentrations (2 mM), highly colored intermediates may limit light

Table 1. Representative Ligands (Grouped by Class) Screened in Heteroleptic $[\text{Co}(\text{LL})_2\text{pyCl}]$ Complexes, with Maximum H_2 Production in Micromoles for Reactions Run at Optimal Conditions (1 equiv CoCl_2 , 2 equiv LL, 1 equiv py) for 1000 min^a

Glyoximes	 GL1 – 15.6	 GL4 – 12.2	 GL14 – 0.3	 GL15 – 0.3
Bipyridines and Phenanthrolines	 BP1 – 0.3	 BP3 – 0.4	 BP4 – 0.5	 BP6 – 0.8
Hydroxyquinolines	 HQ1 – 0.3	 HQ5 – 0.4	 HQ8 – 0.4	 HQ10 – 0.4
Hydrogen Bond Donor Nitrogen Heterocycles	 NH1 – 0.2	 NH2 – 0.4	 NH4 – 0.3	 NH5 – 0.2
Miscellaneous	 MC2 – 0.0	 MC3 – 0.0	 MC4 – 0.0	 MC6 – 0.3

^aSee the Supporting Information for a complete list of ligands used in this study and a comprehensive list of experimental results.

absorption and increase the likelihood of known bimolecular degradation pathways.⁵⁴ We next compared hydrogen production as a relationship between WRC and EY concentrations (Figures 3c and S3). Hydrogen formation demonstrated a considerably higher dependence on WRC rather than EY concentration, suggesting that turnover at the cobalt co-catalyst was slower than photosensitization. Optimal EY and WRC concentrations of 0.6 and 1.2 mM, respectively, were selected at the greatest rate averaged across nonzero concentrations of the inverse component.

We also expected pH to affect the performance of both the WRC and the photosensitizer. The operation of cobaloxime WRCs is pH-dependent,²² and the fluorescence quantum yield and lifetime of EY are the highest above pH 4 (EY $\text{pK}_a = 3.8$).^{11,55} Indeed, the deprotonated, quinoid form of EY^{2-} (Figure 1a) is suggested to be the photoactive form.^{11,12} Hydrogen evolution reactions were performed at varied pH, modified by the addition of potassium hydroxide or hydrochloric acid, and displayed activity independent of WRC concentration (Figures 3e and S4). Above an upper pH limit of ~ 10 , no hydrogen was produced, while below pH 7.5, a substantial precipitate, assigned to the protonated reductant (TEOA, $\text{pK}_a = 7.76$), formed. Small amounts of generated hydrogen at pH 7.5 are consistent with previous reports that protonation of TEOA makes it an ineffective electron donor.^{16,32} The optimal calculated pH, 8.4, was only slightly lower than the inherent pH of prepared solutions (~ 8.9 due to the addition of TEOA) and was consequently unaltered to ease high-throughput reaction preparation. It is notable, however,

that the optimized reaction parameters here are for the parent complex. Some other Co WRCs are known to operate under different ideal conditions, particularly at lower pH.²⁶

Using the optimized reaction conditions, a uniform plate was tested as a means of determining the well-to-well error of the detection system. The average generated H_2 across a 96-well plate was $16.0 \pm 1.3 \mu\text{mol}$, corresponding to a well-to-well error of 8.2% (Figure S5). Control reactions confirmed that photosensitizer, WRC, and light were all necessary to produce hydrogen (Figure S6). Mercury poisoning tests in both screening scale and 10 \times screening scale confirmed that this reaction proceeds without the formation or significant catalytic contribution of cobalt colloids (Figures S8 and S9 and Table S3).

Ligand Screening. We began screening for new molecular cobalt WRCs using our optimized high-throughput platform. Importantly, our reaction parameters are optimized for homoleptic cobaloxime complexes and alternative Co WRCs are known to perform better in different solvents and at lower pH. As other studies have varied the axial monodentate ligand in cobaloxime WRCs,^{29,56,57} we instead focused on exploring the effect of equatorial ligands other than the common dimethylglyoxime.^{7,15,16,30,32,58,59} Heteroleptic complexes of the type $[\text{Co}(\text{LL})_2\text{pyCl}]$ were prepared *in situ* by combining aliquots of stock solutions containing bidentate ligands (LL), CoCl_2 , and pyridine as the consistent axial monodentate ligand. We initially screened 46 different bidentate ligands grouped into discreet classes, including glyoximes (GL), bipyridines and phenanthrolines (BP), 8-hydroxyquinolines (HQ), nitrogen

heterocycles with hydrogen-bond donors (NH), and miscellaneous ligands not readily sorted into another class (MC). Perhaps unsurprisingly, glyoximes were significantly more active than any other ligand, producing the most hydrogen over 1000 min (Tables 1 and S1). Alkyl functionalization, such as that in the archetypal dimethylglyoxime (GL1), was important for hydrogen production, while conjugated glyoxime derivatives and most other ligands generated, at best, only trace amounts of hydrogen.

Selected cobalt WRCs synthesized in batch were assessed for hydrogen production by gas chromatography (Table S2) to confirm the validity of results obtained using complexes synthesized *in situ*. A comparison of these results with high-throughput screening revealed a close correlation between the two techniques. For instance, the WRC containing the deprotonated glyoxime ligand GL2 displayed 86% of the activity compared to the analogous GL1 complex in batch and displayed 90% activity in the high-throughput screen. Homoleptic tris-complexes of BP1 and GL1 are reported as successful WRCs;^{17,54} we also investigated whether these complexes were being made *in situ* rather than the desired [Co(LL)₂pyCl] geometry. *In situ* prepared WRCs incorporating either 2 or 3 equiv of GL1, GL2, and BP1 (and no pyridine) were run in a large number of replicates and compared with previously synthesized [Co(BP1)₃]Cl₂ (Figure 4).⁵⁴ All complexes containing 2,2'-bipyridine (BP1) produced

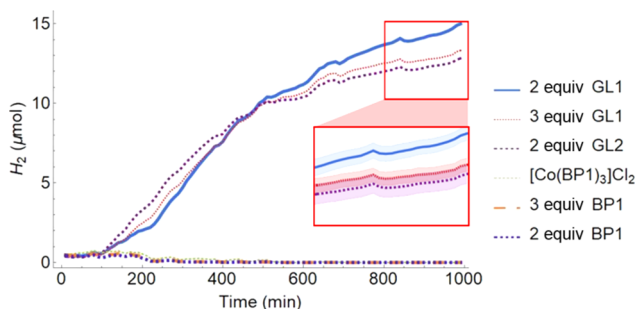


Figure 4. Hydrogen production over time of select cobalt WRCs. Each trace represents the mean of 12 replicates. Inset: standard error represented by the shaded region surrounding each trace. All samples except for [Co(BP1)₃]Cl₂ were prepared *in situ* according to high-throughput screening protocols.

negligible hydrogen, suggesting that differences in our experimental design rendered this WRC inactive for hydrogen production. While [Co(GL1)₃] also produced hydrogen (13.4 μmol), reduced volumes compared to the heteroleptic complex confirmed that we were generating the expected WRC ([Co(GL1)₂pyCl]) under high-throughput conditions.

To further understand the differentiation in the function of homoleptic glyoxime complexes, we performed DFT on several known reaction intermediates using the B3LYP functional and 6-31G(d,p) basis set. The intermediates Co(II)H₂O(GL)₂py, Co(II)(GL)₂py, Co(III)H(GL)₂py, and Co(II)H₂(GL)₂py were explored for all tested glyoximes expected to form a five-member coordinating ring. It is notable that in these calculations, doubly reduced Co(I)H₂O(GL)₂py does not converge, suggesting that water is not a stable ligand, and thus reduction opens an active species for Co(I). This is consistent with the literature.⁶⁰ The free-energy change was estimated according to eq 1 for the binding of a hydride, using the heat of formation determined for each complex and any needed

stoichiometric corrections. This measure of hydride affinity was then compared to the hydrogen produced via the bis-glyoxime complexes. An exponential curve was then fitted to the data ($R^2 = 0.92$), revealing that more negative hydride affinity also results in greater hydrogen production (Figure 5).

$$\begin{aligned} \text{Hydride Affinity} = & \Delta H_f(\text{Co(III)H(GL)}_2\text{py}) \\ & - (\Delta H_f(\text{Co(I)(GL)}_2\text{py}) + \Delta H_f(\text{H}^-)) \end{aligned} \quad (1)$$

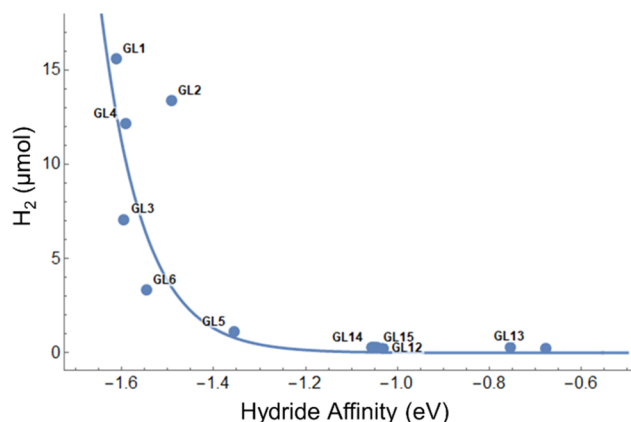


Figure 5. Hydride binding affinity as determined through DFT compared to catalytic production as measured through the parallel reaction system. The fitted curve is of the form $y = a \times b^x$ and presents a correlation coefficient of 0.925.

Knowing that glyoximes were necessary to achieve hydrogen production, we next screened heteroleptic complexes of the type [Co(GL)(LL)pyCl], that is, combining all 46 ligands with each of the 16 glyoximes in an equimolar ratio (Figure 6). Once again, significant amounts of hydrogen were produced only when the WRC contained at least one alkyl-substituted glyoxime ligand (GL1, GL2, GL4, and GL6). Furthermore, in most cases where the *in situ* WRC contained at least 1 equiv of the four active glyoximes, hydrogen was produced independent of the other ligand; only selected ligands (GL11, GL12, MC3, and MC4) completely poisoned the WRC activity. We were mindful that our high-throughput approach was not able to discern the catalytically active species; kinetic or thermodynamic factors may instead lead to appreciable amounts of [Co(GL)₂pyCl] or [Co(LL)₂pyCl] rather than the desired [Co(GL)(LL)pyCl].⁴⁵ Our initial ligand screen revealed that glyoximes were critical for hydrogen production, and we consequently limited our hit selection to ligand combinations that produced >50% of the hydrogen generated using the corresponding [Co(GL)₂pyCl] complex (Tables 1 and S1). This ensured that we did not mistakenly assign activity afforded by a smaller amount of [Co(GL)₂pyCl] present in solution (up to a maximum of 0.5 equiv of expected cobalt WRC).

Heteroleptic complexes that contained 8-hydroxyquinolines (HQ) achieved greater hydrogen evolution than this 50% benchmark (of the corresponding bis-glyoxime WRC) when combined with the active glyoxime ligands (GL1, GL2, GL4, and GL6) except for the nitro-substituted derivative (HQ3). The sulfoxyl-containing HQ2 was particularly active, generating 16.3 μmol over the tested time when combined with GL1, which compares well to the 15.6 μmol observed with the bis-

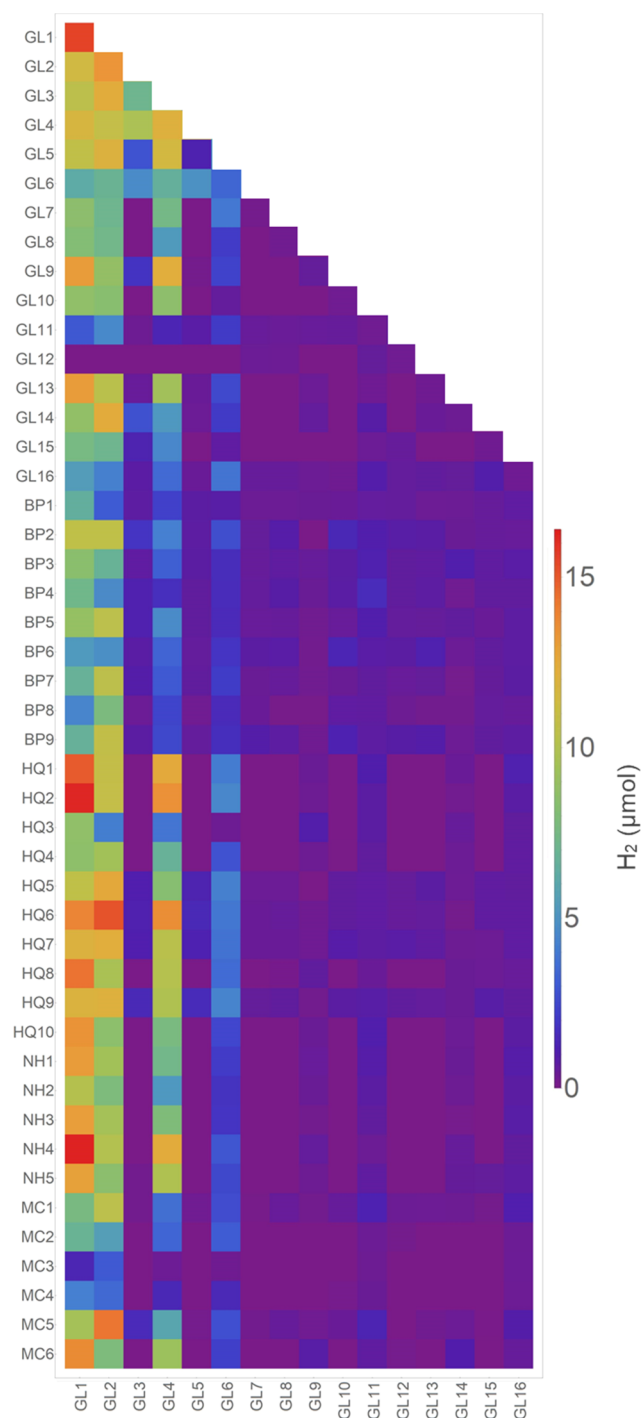


Figure 6. Combinatorial screen of $[\text{Co}(\text{GL})(\text{LL})\text{pyCl}]$ co-catalysts for maximum hydrogen production in micromoles for reactions run at optimal conditions (1 equiv CoCl_2 , 1 equiv GL, 1 equiv LL, 1 equiv py) for 1000 min.

GL1 analogue (Figure 6). Ligands with nitrogen-containing heterocycles capable of acting as hydrogen-bond donors also performed above the benchmark in almost all cases when combined with GL1, GL2, and GL4. The *in situ* formed complex $[\text{Co}(\text{GL1})(\text{NH4})\text{pyCl}]$ evolved the most hydrogen of all of the screened compounds, $16.4 \mu\text{mol}$ (Figure 6). The primary amine-containing ligands 2,3-diaminonaphthalene (MC5) and 8-aminoquinoline (MC6) also demonstrated

moderate activity (14.4 and $13.7 \mu\text{mol H}_2$, respectively) in combination with select alkyl glyoximes.

Replicate reactions of $[\text{Co}(\text{GL1})(\text{NH4})\text{pyCl}]$ and $[\text{Co}(\text{GL1})(\text{HQ2})\text{pyCl}]$ confirmed that these ligand combinations reproducibly evolved significant amounts of hydrogen (Figure S7). Interestingly, all well-performing ligands (above the 50% benchmark) contain functional groups that serve as hydrogen-bond donors. The catalytic cycle of cobaloximes is complex, and both mono- and bimolecular pathways are reported; however, it is plausible that hydrogen bonding in equatorial glyoximes facilitates the proton-coupled electron transfer required to form the cobalt hydride intermediate critical for hydrogen evolution.²⁸ Our results strengthen the argument that hydrogen bonding plays an important role in facilitating water reduction in cobalt-based WRCs. Electron donating axial ligands, such as substituted pyridines and imidazoles, in bis-glyoxime complexes also improve catalytic activity, rationalized by an increased electron density and basicity of the protonated intermediate.^{50,55} The improved performance observed specifically with monodentate imidazoles as the axial ligand is notable in comparison to the nitrogen heterocycles present in our NH ligand series, further strengthening the argument that hydrogen bonding plays an important role in facilitating water reduction in cobalt-based WRCs.

CONCLUSIONS

High-throughput experimentation enabled the rapid design and optimization of a homogeneous photocatalytic water reduction method without any noble-metal components. The cobalt-based WRC $[\text{Co}(\text{GL1BF}_2)_2\text{pyCl}]$ demonstrated an optimal catalyst/substrate ratio of 1:7000 molecules of water and was effective across a range of concentrations (0.2–2 mM). An initial screen of 46 different coordinating ligands for *in situ* prepared WRCs revealed that alkyl-substituted glyoximes were critical for hydrogen production in our parallel screening conditions. DFT simulations demonstrated a connection between the hydride affinity and the catalytic performance for these bis-glyoxime species. A larger subsequent combinatorial screen of each glyoxime derivative paired with all other ligands (to give 616 distinct co-catalysts of the type $[\text{Co}(\text{GL})(\text{LL})\text{pyCl}]$) identified several promising ligand classes all containing functional groups that may act as hydrogen-bond donors. Two distinct catalysts, $[\text{Co}(\text{GL1})(\text{HQ2})\text{pyCl}]$ and $[\text{Co}(\text{GL1})(\text{NH4})\text{pyCl}]$, produced greater amounts of hydrogen than the archetypal bis-glyoxime WRC $[\text{Co}(\text{GL1})_2\text{pyCl}]$. Isolation and characterization of these promising candidates, along with their mechanism for producing hydrogen, are currently being investigated.

ASSOCIATED CONTENT

Supporting Information

The Supporting Information is available free of charge at <https://pubs.acs.org/doi/10.1021/acs.inorgchem.0c02790>.

Reagents used, synthetic procedures, and characterization for glyoxime derivative ligands and fully synthesized cobalt glyoxime complexes; further description of photoreactor design and use; detailed experimental information and results for optimization experiments; results of control testing and uniform reactions; full results from homoleptic ligand screening and associated ligand structures; and experimental details

and gas chromatography analysis of larger-scale experiments (PDF)
Heteroleptic screening data (XLSX)

AUTHOR INFORMATION

Corresponding Author

Stefan Bernhard – Department of Chemistry, Carnegie Mellon University, Pittsburgh, Pennsylvania 15213, United States;
orcid.org/0000-0002-8033-1453; Email: bern@cmu.edu

Authors

Rachel N. Motz – Department of Chemistry, Carnegie Mellon University, Pittsburgh, Pennsylvania 15213, United States
Eric M. Lopato – Department of Chemistry, Carnegie Mellon University, Pittsburgh, Pennsylvania 15213, United States
Timothy U. Connell – Department of Chemistry, Carnegie Mellon University, Pittsburgh, Pennsylvania 15213, United States;
orcid.org/0000-0002-6142-3854

Complete contact information is available at:
<https://pubs.acs.org/10.1021/acs.inorgchem.0c02790>

Notes

The authors declare no competing financial interest.

ACKNOWLEDGMENTS

S.B. gratefully acknowledges National Science Foundation (NSF) funding CHE 1764353 for this work. Seed funding for the development of the high-throughput reactors came from Carnegie Mellon University's Kavcic-Moura Fund and Manufacturing Futures Initiative. E.M.L. was supported by the Steinbrenner Institute Graduate Fellowship and the ARCS Foundation Pittsburgh Chapter. T.U.C. was supported by a Fulbright Future Scholarship. Seed code used to generate the image analysis program was provided by Tomasz Kowalewski.

REFERENCES

- (1) Climate Change 2014: Mitigation of Climate Change. Contribution of Working Group III to the Fifth Assessment Report of the Intergovernmental Panel on Climate Change; IPCC: Cambridge, UK and New York, NY, 2014.
- (2) Ogden, J. M. Prospects For Building A Hydrogen Energy Infrastructure. *Annu. Rev. Energy Environ.* **1999**, *24*, 227–279.
- (3) Technical Support Document For Hydrogen Production: Proposed Rule For Mandatory Reporting of Greenhouse Gases; Office of Air and Radiation, US EPA, 2008.
- (4) McDaniel, N. D.; Bernhard, S. Solar fuels: thermodynamics, candidates, tactics, and figures of merit. *Dalton Trans.* **2010**, *39*, 10021–10030.
- (5) Tachibana, Y.; Vayssieres, L.; Durrant, J. R. Artificial photosynthesis for solar water-splitting. *Nat. Photonics* **2012**, *6*, 511–518.
- (6) Curtin, P. N.; Tinker, L. L.; Burgess, C. M.; Cline, E. D.; Bernhard, S. Structure-activity correlations among iridium(III) photosensitizers in a robust water-reducing system. *Inorg. Chem.* **2009**, *48*, 10498–10506.
- (7) Fihri, A.; Artero, V.; Pereira, A.; Fontecave, M. Efficient H₂-producing photocatalytic systems based on cyclometalated iridium- and tricarbonylrhenium-diimine photosensitizers and cobaloxime catalysts. *Dalton Trans.* **2008**, 5567–5569.
- (8) Chirdon, D. N.; Transue, W. J.; Kagalwala, H. N.; Kaur, A.; Maurer, A. B.; Pintauer, T.; Bernhard, S. [Ir(NANAN)(CAN)L]⁺: a new family of luminophores combining tunability and enhanced photostability. *Inorg. Chem.* **2014**, *53*, 1487–1499.
- (9) Mills, I. N.; Kagalwala, H. N.; Chirdon, D. N.; Brooks, A. C.; Bernhard, S. New Ir(III) 4,4'-dicyano-2,2'-bipyridine photosensitizers for solar fuel generation. *Polyhedron* **2014**, *82*, 104–108.
- (10) Wang, M.; Na, Y.; Gorlov, M.; Sun, L. Light-driven hydrogen production catalysed by transition metal complexes in homogeneous systems. *Dalton Trans.* **2009**, 6458–6467.
- (11) Majek, M.; Filace, F.; von Wangelin, A. J. On the mechanism of photocatalytic reactions with eosin Y. *Beilstein J. Org. Chem.* **2014**, *10*, 981–989.
- (12) Majek, M.; von Wangelin, A. J. Mechanistic Perspectives on Organic Photoredox Catalysis for Aromatic Substitutions. *Acc. Chem. Res.* **2016**, *49*, 2316–2327.
- (13) Misawa, H.; Sakuragi, H.; Usui, Y.; Tokumaru, K. Photosensitizing Action of Eosin Y for Visible Light Induced Hydrogen Evolution from Water. *Chem. Lett.* **1983**, *12*, 1021–1024.
- (14) Li, D.; Wehrung, J.-F.; Zhao, Y. Gold nanoparticle-catalysed photosensitized water reduction for hydrogen generation. *J. Mater. Chem. A* **2015**, *3*, 5176–5182.
- (15) Lazarides, T.; McCormick, T.; Du, P.; Luo, G.; Lindley, B.; Eisenberg, R. Making Hydrogen from Water Using a Homogeneous System Without Noble Metals. *J. Am. Chem. Soc.* **2009**, *131*, 9192–9194.
- (16) Wang, Z. Y.; Rao, H.; Deng, M. F.; Fan, Y. T.; Hou, H. W. Photocatalytic H₂ generation based on noble-metal-free binuclear cobalt complexes using visible-light. *Phys. Chem. Chem. Phys.* **2013**, *15*, 16665–16671.
- (17) Du, P.; Eisenberg, R. Catalysts made of earth-abundant elements (Co, Ni, Fe) for water splitting: Recent progress and future challenges. *Energy Environ. Sci.* **2012**, *5*, 6012–6021.
- (18) Call, A.; Franco, F.; Kandoth, N.; Fernandez, S.; Gonzalez-Bejar, M.; Perez-Prieto, J.; Luis, J. M.; Lloret-Fillol, J. Understanding light-driven H₂ evolution through the electronic tuning of aminopyridine cobalt complexes. *Chem. Sci.* **2018**, *9*, 2609–2619.
- (19) Li, C.-B.; Gong, P.; Yang, Y.; Wang, H.-Y. Cobalt(II)–Salen Complexes for Photocatalytic Hydrogen Production in Noble Metal-Free Molecular Systems. *Catal. Lett.* **2018**, *148*, 3158–3164.
- (20) Dempsey, J. L.; Brunswig, B. S.; Winkler, J. R.; Gray, H. B. Hydrogen Evolution Catalyzed by Cobaloximes. *Acc. Chem. Res.* **2009**, *42*, 1995–2004.
- (21) Solis, B. H.; Hammes-Schiffer, S. Theoretical analysis of mechanistic pathways for hydrogen evolution catalyzed by cobaloximes. *Inorg. Chem.* **2011**, *50*, 11252–11262.
- (22) Muckerman, J. T.; Fujita, E. Theoretical studies of the mechanism of catalytic hydrogen production by a cobaloxime. *Chem. Commun.* **2011**, *47*, 12456–12458.
- (23) Artero, V.; Saveant, J. M. Toward the Rational Benchmarking of Homogeneous H₂-Evolving Catalysts. *Energy Environ. Sci.* **2014**, *7*, 3808–3814.
- (24) Bhattacharjee, A.; Andreiadis, E. S.; Chavarot-Kerlidou, M.; Fontecave, M.; Field, M. J.; Artero, V. A computational study of the mechanism of hydrogen evolution by cobalt(diimine-dioxime) catalysts. *Chem. – Eur. J.* **2013**, *19*, 15166–15174.
- (25) Dempsey, J. L.; Winkler, J. R.; Gray, H. B. Mechanism of H₂ Evolution from a Photogenerated Hydridocobaloxime. *J. Am. Chem. Soc.* **2010**, *132*, 16774–16776.
- (26) Jacques, P.-A.; Artero, V.; Pécaut, J.; Fontecave, M. Cobalt and nickel diimine-dioxime complexes as molecular electrocatalysts for hydrogen evolution with low overvoltages. *Proc. Natl. Acad. Sci. U.S.A.* **2009**, *106*, 20627–20632.
- (27) Chen, J.; Sit, P. H. Density Functional Theory and Car-Parrinello Molecular Dynamics Study of the Hydrogen-Producing Mechanism of the Co(dmgbF₂)₂ and Co(dmgh)₂ Cobaloxime Complexes in Acetonitrile-Water Solvent. *J. Phys. Chem. A* **2017**, *121*, 3515–3525.
- (28) Jiang, Y.-K.; Liu, J.-H. DFT studies of cobalt hydride intermediate on cobaloxime-catalyzed H₂ evolution pathways. *Int. J. Quantum Chem.* **2012**, *112*, 2541–2546.
- (29) Razavet, M.; Artero, V.; Fontecave, M. Proton Electoreduction Catalyzed by Cobaloximes: Functional Models for Hydrogenases. *Inorg. Chem.* **2005**, *44*, 4786–4795.
- (30) Zhang, P.; Wang, M.; Dong, J.; Li, X.; Wang, F.; Wu, L.; Sun, L. Photocatalytic Hydrogen Production from Water by Noble-Metal-

Free Molecular Catalyst Systems Containing Rose Bengal and the Cobaloximes of BF_x-Bridged Oxime Ligands. *J. Phys. Chem. C* **2010**, *114*, 15868–15874.

(31) Solis, B. H.; Hammes-Schiffer, S. Substituent effects on cobalt diglyoxime catalysts for hydrogen evolution. *J. Am. Chem. Soc.* **2011**, *133*, 19036–19039.

(32) Du, P.; Knowles, K.; Eisenberg, R. A Homogeneous System for the Photogeneration of Hydrogen from Water Based on a Platinum(II) Terpyridyl Acetylide Chromophore and a Molecular Cobalt Catalyst. *J. Am. Chem. Soc.* **2008**, *130*, 12576–12577.

(33) Kwok, C. L.; Cheng, S. C.; Ho, P. Y.; Yiu, S. M.; Man, W. L.; Au, V. K.; Tsang, P. K.; Leung, C. F.; Ko, C. C.; Robert, M. Precious-metal free photocatalytic production of an NADH analogue using cobalt diimine-dioxime catalysts under both aqueous and organic conditions. *Chem. Commun.* **2020**, 7491–7494.

(34) Dolui, D.; Khandelwal, S.; Majumder, P.; Dutta, A. The odyssey of cobaloximes for catalytic H₂ production and their recent revival with enzyme-inspired design. *Chem. Commun.* **2020**, 56, 8166–8181.

(35) Cao, S.; Piao, L. Considerations for a More Accurate Evaluation Method for Photocatalytic Water Splitting. *Angew. Chem., Int. Ed.* **2020**, *59*, 18312–18320.

(36) Cawse, J. N. Experimental Strategies for Combinatorial and High-Throughput Materials Development. *Acc. Chem. Res.* **2001**, *34*, 213–221.

(37) Kumar, R. A.; Clark, D. S. High-throughput screening of biocatalytic activity: applications in drug discovery. *Curr. Opin. Chem. Biol.* **2006**, *10*, 162–168.

(38) Krska, S. W.; DiRocco, D. A.; Dreher, S. D.; Shevlin, M. The Evolution of Chemical High-Throughput Experimentation To Address Challenging Problems in Pharmaceutical Synthesis. *Acc. Chem. Res.* **2017**, *50*, 2976–2985.

(39) Nursam, N. M.; Wang, X.; Caruso, R. A. High-Throughput Synthesis and Screening of Titania-Based Photocatalysts. *ACS Comb. Sci.* **2015**, *17*, 548–569.

(40) Bai, Y.; Wilbraham, L.; Slater, B. J.; Zwijnenburg, M. A.; Sprick, R. S.; Cooper, A. I. Accelerated Discovery of Organic Polymer Photocatalysts for Hydrogen Evolution from Water through the Integration of Experiment and Theory. *J. Am. Chem. Soc.* **2019**, *141*, 9063–9071.

(41) Sawada, K.; Nakajima, T. High-throughput screening of perovskite oxynitride and oxide materials for visible-light photocatalysis. *APL Mater.* **2018**, *6*, No. 101103.

(42) Wu, Y.; Lazic, P.; Hautier, G.; Persson, K.; Ceder, G. First principles high throughput screening of oxynitrides for water-splitting photocatalysts. *Energy Environ. Sci.* **2013**, *6*, 157–168.

(43) Lopato, E. M.; Eikey, E. A.; Simon, Z. C.; Back, S.; Tran, K.; Lewis, J.; Kowalewski, J. F.; Yazdi, S.; Kitchin, J. R.; Ulissi, Z. W.; Millstone, J. E.; Bernhard, S. Parallelized Screening of Characterized and DFT-Modeled Bimetallic Colloidal Cocatalysts for Photocatalytic Hydrogen Evolution. *ACS Catal.* **2020**, *10*, 4244–4252.

(44) Song, W.; Lopato, E. M.; Bernhard, S.; Salvador, P. A.; Rohrer, G. S. High-throughput measurement of the influence of pH on hydrogen production from BaTiO₃/TiO₂ core/shell photocatalysts. *Appl. Catal., B* **2020**, *269*, No. 118750.

(45) Renom-Carrasco, M.; Lefort, L. Ligand libraries for high throughput screening of homogeneous catalysts. *Chem. Soc. Rev.* **2018**, *47*, 5038–5060.

(46) Chugunova, E.; Samsonov, V.; Akyzbekov, N.; Mazhukin, D. Synthesis of 2H-benzimidazole 1,3-dioxides, separase inhibitors, by reaction of o-benzoquinone dioximes with ketones. *Tetrahedron* **2017**, *73*, 3986–3992.

(47) Bookser, B. C. 2-Benzylloxymethyl-5-(tributylstannyl)tetrazole. A reagent for the preparation of 5-aryl- and 5-heteroaryl-1H-tetrazoles via the Stille reaction. *Tetrahedron Lett.* **2000**, *41*, 2805–2809.

(48) Lân, N. M.; Burgard, R.; Wentrup, C. Rearrangement of 2-Quinolyl- and 1-Isoquinolylcarbenes to Naphthyl nitrenes. *J. Org. Chem.* **2004**, *69*, 2033–2036.

(49) Colombo, A.; Dragonetti, C.; Magni, M.; Meroni, D.; Ugo, R.; Marotta, G.; Grazia Lobello, M.; Salvatori, P.; De Angelis, F. New

thiocyanate-free ruthenium(II) sensitizers with different pyrid-2-yl tetrazolate ligands for dye-sensitized solar cells. *Dalton Trans.* **2015**, *44*, 11788–11796.

(50) Yang, T.; Chen, G.; Sang, Z.; Liu, Y.; Yang, X.; Chang, Y.; Long, H.; Ang, W.; Tang, J.; Wang, Z.; Li, G.; Yang, S.; Zhang, J.; Wei, Y.; Luo, Y. Discovery of a Teraryl Oxazolidinone Compound (S)-N-((3-(3-Fluoro-4-(4-(pyridin-2-yl)-1H-pyrazol-1-yl)phenyl)-2-oxooxazolidin-5-yl)methyl)acetamide Phosphate as a Novel Antimicrobial Agent with Enhanced Safety Profile and Efficacies. *J. Med. Chem.* **2015**, *58*, 6389–6409.

(51) Schrauzer, G. N. Bis(dimethylglyoximate)Cobalt Complexes. In *Inorganic Syntheses*; Jolly, W. L., Ed.; McGraw-Hill Book Company, Inc.: New York, NY, 1968; Vol. XI, pp 61–70.

(52) Hadjmohammadi, M. R.; Chaichi, M. J.; Yousefpour, M. Solvatochromism Effect of Different Solvents on UV-Vis Spectra of Fluorescein and its Derivatives. *Iran. J. Chem. Chem. Eng.* **2008**, *27*, 9–14.

(53) Chakraborty, M.; Panda, A. K. Spectral behaviour of eosin Y in different solvents and aqueous surfactant media. *Spectrochim. Acta, Part A* **2011**, *81*, 458–465.

(54) Goldsmith, J. I.; Hudson, W. R.; Lowry, M. S.; Anderson, T. H.; Bernhard, S. Discovery and High-Throughput Screening of Heteroleptic Iridium Complexes for Photoinduced Hydrogen Production. *J. Am. Chem. Soc.* **2005**, *127*, 7502–7510.

(55) Slyusareva, E. A.; Gerasimova, M. A. pH-Dependence of the Absorption and Fluorescent Properties of Fluorone Dyes in Aqueous Solutions. *Russ. Phys. J.* **2014**, *56*, 1370–1377.

(56) Panagiotopoulos, A.; Ladomenou, K.; Sun, D.; Artero, V.; Coutsolelos, A. G. Photochemical hydrogen production and cobaloximes: the influence of the cobalt axial N-ligand on the system stability. *Dalton Trans.* **2016**, *45*, 6732–6738.

(57) Wakerley, D. W.; Reisner, E. Development and understanding of cobaloxime activity through electrochemical molecular catalyst screening. *Phys. Chem. Chem. Phys.* **2014**, *16*, 5739–5746.

(58) Connolly, P.; Espenson, J. H. Cobalt-Catalyzed Evolution of Molecular Hydrogen. *Inorg. Chem.* **1986**, *25*, 2684–2688.

(59) Bakac, A.; Espenson, J. H. Unimolecular and Bimolecular Homolytic Reactions of Organochromium and Organocobalt Complexes. Kinetics and Equilibria. *J. Am. Chem. Soc.* **1984**, *106*, 5197–5202.

(60) Bhattacharjee, A.; Chavarot-Kerlidou, M.; Dempsey, J. L.; Gray, H. B.; Fujita, E.; Muckerman, J. T.; Fontecave, M.; Artero, V.; Arantes, G. M.; Field, M. J. Theoretical modeling of low-energy electronic absorption bands in reduced cobaloximes. *ChemPhysChem* **2014**, *15*, 2951–2958.